



A novel dual-modality imaging agent targeting folate receptor of tumor for molecular imaging and fluorescence-guided surgery

Myoung Hyoun Kim¹ · Seul-Gi Kim² · Dae-Weung Kim^{1,2}

Received: 21 March 2019 / Accepted: 19 May 2019 / Published online: 27 May 2019
© The Japanese Society of Nuclear Medicine 2019

Abstract

Objective Folate receptor (FR) is an ideal target for cancer imaging because it is frequently overexpressed in major types of human tumor, whereas its expression in normal organs is highly limited. Combining nuclear and fluorescence-imaging techniques provides a novel approach for cancer imaging and monitoring the surgery. The objective of this study was to report the synthesis and characteristics of a dual-modality imaging agent, Tc-99m Folate-Gly-His-Glu-Gly-Glu-Cys-Gly-Lys(-5-carboxy-X-rhodamine)-NH₂ (Folate-ECG-ROX), and verify its feasibility as both molecular imaging agent and intra-operative guidance.

Methods Folate-ECG-ROX was synthesized using Fmoc solid-phase peptide synthesis. Radiolabeling of Folate-ECG-ROX with Tc-99m was done using ligand exchange via tartrate. Binding affinity and in vitro cellular uptake studies were performed. Gamma camera imaging, biodistribution and ex vivo imaging studies were performed using KB and HT-1080 tumor-bearing murine models. Tumor tissue slides were prepared and analyzed with immunohistochemistry staining and confocal microscopy. Surgical removal of tumor nodules in murine models with peritoneal carcinomatosis was performed under the fluorescence-imaging system.

Results After radiolabeling procedures with Tc-99m, Tc-99m Folate-ECG-ROX complexes were prepared in high yield (> 97%). The binding affinity value (K_d) of Tc-99m Folate-ECG-ROX for KB cells was estimated to be 6.9 ± 0.9 nM. In gamma camera imaging, tumor to normal muscle uptake ratio of Tc-99m Folate-ECG-ROX increased with time (3.4 ± 0.4 , 4.4 ± 0.7 , and 6.6 ± 0.8 at 1, 2, and 3 h, respectively). In biodistribution study, %IA/g for KB tumor was 2.50 ± 0.80 and 4.08 ± 1.16 at 1 and 3 h, respectively. Confocal microscopy with immunohistochemistry staining detected strong Tc-99m Folate-ECG-ROX fluorescence within KB tumor tissue which is correlating with the fluorescent activity of anti-FR antibody. Under real-time optical imaging, the removal of visible nodules was successfully performed.

Conclusions In vivo and in vitro studies revealed substantial and specific uptake of Tc-99m Folate-ECG-ROX in FR-positive tumors. Thus, Tc-99m Folate-ECG-ROX could provide both pre-operative molecular imaging and fluorescence image-guidance for tumor.

Keywords Folate · Tc-99m · ROX · Multimodal imaging · Fluorescence-guided surgery

Electronic supplementary material The online version of this article (<https://doi.org/10.1007/s12149-019-01369-2>) contains supplementary material, which is available to authorized users.

✉ Dae-Weung Kim
akaxan@nate.com

¹ Department of Nuclear Medicine and Institute of Wonkwang Medical Science, Wonkwang University School of Medicine, 344-2 Shinyong-Dong, Iksan, Jeollabuk-do 570-711, Republic of Korea

² Research Unit of Molecular Imaging Agent (RUMIA), Wonkwang University School of Medicine, 344-2 Shinyong-Dong, Iksan, Jeollabuk-do 570-711, Republic of Korea

Introduction

Multimodality imaging, a combination of two or more imaging modalities, may provide a better solution for imaging than individual techniques [1]. An imaging agent that can combine a radionuclide and a near-infrared fluorescent dye is highly desirable for dual nuclear and fluorescent imaging [2]. Nuclear imaging, an established clinical imaging modality, covers the whole body and offers excellent sensitivity and penetration. However, nuclear imaging techniques are limited by relatively long acquisition time and poor spatial resolution. Although fluorescent imaging offers real-time

and high-resolution images, it is limited by the poor tissue penetration [3]. A combination of nuclear and fluorescent imaging techniques might offer synergistic advantages over single modality.

Dual nuclear and fluorescent imaging agent targeting cancer tissue could play a major role in cancer surgery. Pre-operatively, nuclear imaging allows determination of cancer stage and surgical extent. This is the classic role of molecular imaging in cancer surgery. Intra-operatively, optical imaging could provide surgical guidance and allow immediate differentiation between normal and diseased tissues beyond gross anatomical distortion or discoloration [4]. This can offer more complete removal of diseased tissue with minimal inadvertent injury to vital structures [5]. Post-operatively, nuclear imaging could assure surgical completeness. It would be more useful when portable gamma camera system is used in the operation room [6].

For this application, high-binding affinity and specificity of dual-modality imaging agent for cancer is requisite. Folate receptor (FR) is ideally suited for this use because it is frequently overexpressed in major types of human tumors (including ovary, lung, breast and colon) whereas its expression in normal organs except the kidneys is highly limited [7]. Thus, FR has been used as a target for selective delivery of drugs to these tumors such as radiopharmaceuticals, magnetic resonance imaging (MRI) contrast agents, chemotherapeutic agents, antisense oligonucleotides, protein toxins, and liposomes with entrapped drugs [8].

In the present study, we developed Tc-99m Folate-Gly-His-Glu-Gly-Glu-Cys-Gly-Lys(-5-carboxy-X-rhodamine)-NH₂ (Folate-ECG-ROX) as a dual-modality imaging agent to target FR-positive tumor cells. Simultaneous labeling with Tc-99m and ROX could provide both nuclear and fluorescent imaging. The diagnostic performance and surgical usage of Tc-99m Folate-ECG-ROX as a dual-modality imaging agent for tumor was also evaluated in a murine model.

Materials and methods

Materials

Folic acid dihydrate, 1N-HCl, acetone, SnCl₂, and sodium tartrate were purchased from Sigma-Aldrich Korea (Seoul, Korea). 5-Carboxy-X-rhodamine, succinimidyl ester (5-ROX, SE) was purchased from ChemPep, Inc. (Wilmington, FL, USA). Tc-99m pertechnetate was eluted from a commercial technetium generator (Tyco Healthcare, Mallinckrodt, Dublin, Ireland) at our institution. Instant thin-layer chromatography-silica gel (ITLC-SG) capillary column was purchased from Futurechem (Seoul, Korea). KB human squamous carcinoma (FR-positive) and HT-1080

fibrosarcoma (FR negative) cell lines were obtained from the Korean Cell Line Bank (Seoul, Korea).

Synthesis and characterization of Folate-ECG-ROX

Folate-ECG-ROX with purity >96% was synthesized commercially by Anygen, Inc. (Gwangju, Korea). Briefly, peptides were synthesized using Fmoc solid-phase peptide synthesis (SPPS). The resulting peptide-bound resin was treated with folic acid dihydrate in dimethyl sulfoxide (DMSO) and 2 M hydroxybenzotriazole (HOBt)/2 M *N,N'*-diisopropylcarbodiimide (DIC). After 4 h of incubation, 5-ROX, SE in *N,N*-dimethylformamide (DMF) and 2 M *N,N*-diisopropylethylamine (DIEA) were added and incubated at room temperature for 24 h. The synthesized compound was purified using reverse phase high-performance liquid chromatography (RP-HPLC) with a Shimadzu C18 analytical column (C18, 5 μm, 100 Å column, 4.6×250 mm). Linear gradient from 0 to 70% acetonitrile in water containing 0.1% trifluoroacetic acid (TFA) was used for elution. Mass was analyzed by mass spectrometry (AXIMA-CFR, MALDI-TOF Mass Spectrometer).

Radiolabeling with Tc-99m

Radiolabeling of Folate-ECG-ROX with Tc-99m was done as described previously [9–11]. Briefly, mixed solution of Folate-ECG-ROX (0.005 mg/ml in 300 μl nitrogen-purged water) and sodium tartrate (100 mg/ml in 300 μl nitrogen-purged water) was prepared in a microcentrifuge tube. This solution was amended with fresh Tc-99m pertechnetate (1.0 ml, about 1110 MBq) and SnCl₂ (1 mg/ml in 30 μl nitrogen-purged 0.01 M HCl). The solution was heated at 95 °C for 15 min and cooled at room temperature. Characterization of radiolabeled Tc-99m Folate-ECG-ROX was done by a system consisting of Gilson 321 HPLC pumps (Gilson, Inc., Middleton, WI, USA), a Bioscan FC-1000 radiodetector (Bioscan, Inc., Washington DC, USA), Trilution LC software (Gilson, Inc.), and YMC-Triart C18 column (4.6×100 nm; YMC, Kyoto, Japan). Solvent A was 0.1% TFA in water and solvent B was 0.1% TFA in acetonitrile. A linear gradient from 0 to 35% solvent B over 35 min was employed at a flow rate of 1 mL/min. Ultraviolet detector (230 nm) and gamma radiodetector were used for monitoring.

The labeled complex (0.1 ml) was incubated at 37 °C with saline (1 ml) at room temperature (25 °C) and freshly collected human serum (1 ml). Samples were withdrawn at 30 min, 1, 3, and 24 h and analyzed using ITLC-SG with saline (*R_f* of Tc-99m Folate-ECG-ROX and free pertechnetate = 0.9–1.0;

R_f of colloid = 0.0–0.1) and acetone (R_f of free pertechnetate = 0.9–1.0; R_f of Tc-99m Folate-ECG-ROX and colloid = 0.0–0.1) as mobile phases. All experiments were conducted in triplicate ($n=3$).

In vitro receptor-binding affinity

KB and HT-1080 cells were cultured in a humidified atmosphere with 5% CO₂. Culture medium was folate-free RPMI 1640 (FFRPMI 1640; Gibco Laboratories, Grand Island, NY, USA) supplemented with 10% fetal bovine serum (FBS), L-glutamine (300 mg/l), 25 mM 4-(2-hydroxyethyl)-1-piperazineethanesulfonic acid (HEPES), and 25 mM NaHCO₃. Binding affinities of Tc-99m Folate-ECG-ROX for KB and HT-1080 cells were determined by saturation binding experiments as described previously [12]. Briefly, KB and HT-1080 cells were seeded into 24-well plates at density of 1×10^6 cells/well and cultured overnight. Cells were washed twice (5 min each) with ice-cold binding buffer (25 mM HEPES and 1% bovine serum albumin [BSA]). A concentration gradient (0–500 nM) of Tc-99m Folate-ECG-ROX was then added to wells and incubated with cells at 37 °C for 1 h. Total volume of each well was 300 μ l. After cells were rinsed twice with ice-cold binding buffer, cells of each well were collected for gamma counting. Radioactivity was measured using a 1480 Wizard 3 gamma counter (PerkinElmer Life and Analytical Sciences, Wallingford, CT, USA). The binding affinity value (K_d) was calculated using non-linear regression models in GraphPad Prism software version 5.03 (GraphPad Software, La Jolla, CA, USA). Each data point is the mean of four determinations.

Cellular uptake using confocal microscopy

KB and HT-1080 cells (1×10^5 cells/well) were cultured on the top of a cover-slip slide at 37 °C for 24 h. The medium was removed and replaced with fresh serum-free medium (500 μ l) containing Tc-99m Folate-ECG-ROX (200 nM). Cells were incubated at 37 °C for 1 h. These cells were washed three times with phosphate-buffered saline (PBS). Cover-slips were placed on slides containing one drop of fluorescent mounting medium (Dako, Glostrup, Denmark). Confocal laser scanning microscopy was performed using a FV1200 confocal microscope (Olympus, Pittsburgh, PA, USA) with a 100 \times oil immersion lens.

Murine models with tumor

Six-week-old female homozygous athymic BALB/c nu/nu mice (weighing 16–18 g) were purchased from Daejeon Science (Daejeon, Korea) and kept in cages. They were provided free access to food and tap water. These mice received

a folate-free diet (TD.95247, Harlan Laboratories, Indianapolis, IN, USA) for 3 weeks to reduce serum folate level to a physiologic range as previously reported [13]. They were then subcutaneously inoculated with 1×10^7 KB (FR positive) and HT-1080 (FR-negative, as an internal reference) cells (0.1 ml PBS) in the right side and left side of anterior chest region, respectively. Tumors were allowed to grow to about 400 to 550 mm³ in volume by caliper measurements of perpendicular dimensions. Approximately 14 days after inoculation, gamma camera imaging, in vivo optical imaging, and biodistribution studies were performed.

In vivo gamma camera imaging and competition study

Tumor-bearing mice were anesthetized by intra-peritoneal injection of ketamine (60 mg/kg)/xylazine (5 mg/kg). Once the animal was in surgical plane of anesthesia, 55.5 MBq (200 nM in 150 μ l) of Tc-99m Folate-ECG-ROX was intravenously administered via tail vein. In vivo imaging was performed at 1, 2, and 3 h after injection using a gamma camera (Vertex; ADAC Laboratories, Milpitas, CA, USA) equipped with a pin-hole collimator. Images were digitally stored in a size of 512 \times 512 matrix. Regions of interest (ROIs, 15 \times 15 pixels) were drawn at sites of tumors on chest walls. Additional ROIs were drawn at the left arm muscle for normal muscle uptake measurement ($n=5$, respectively). Average counts per pixel within ROIs were measured and target to non-target ratios were calculated.

To evaluate whether Tc-99m Folate-ECG-ROX can specifically bind to FR and compete with free folate, an in vivo binding inhibition (competition) study was performed. Tc-99m Folate-ECG-ROX (200 nM) and free folate (4 mM, about 20 times the concentration of Tc-99m Folate-ECG-ROX) were co-injected intravenously via the tail vein ($n=5$). Serial imaging at 1, 2, and 3 h after injection was done as described above.

Ex vivo fluorescent imaging and postmortem studies

Following the in vivo gamma imaging study, mice ($n=5$) were killed. Tumor tissue and several different organs were excised and ex vivo fluorescent imaging study was performed using a fluorescence-imaging system (FOBI-10BR, Neoscience). Emission band for 5-ROX, SE (peak absorbance and peak emission wavelength = 575 and 602 nm, respectively) ranged from 520 to 675 nm. Exposure time was 2.5 s per image. The image was analyzed using dedicated software.

Tumors were divided into two pieces after fluorescent imaging study. Each piece was assigned randomly to either the biodistribution study or the confocal microscopy. Tumor tissue for confocal microscopy was immediately snap-frozen using optimal cutting temperature (OCT) solution.

Biodistribution study

Tissues of tumor and selected organs were weighed and collected into pre-weighed gamma counter tubes. Radioactivities of tissues were counted in a gamma counter (1480 Wizard 3, PerkinElmer Life and Analytical Sciences). Counts per minute were decay-corrected. Results are expressed as a percentage injected activity per gram of wet tissue (%IA/g). Total activities injected per animal were calculated by calculating the difference between initial syringe counts and remaining syringe counts after administration.

Immunohistochemistry staining

Frozen tumor tissues were cut into slices (10 μm in thickness). After thorough drying at room temperature, slices were fixed with ice-cold acetone for 10 min and air dried at room temperature for 20 min. Tumor sections were incubated with 5% goat serum for 30 min at room temperature to block nonspecific binding. Tumor sections were then incubated with mouse anti-FR antibody (sc-5155219, 1:100 dilution; Santa Cruz Biotechnology, Santa Cruz, CA, USA) for 1 h at room temperature. After washing with PBS buffer, tumor slides were incubated with Alexa Fluor[®] 488-conjugated goat anti-mouse secondary antibody (cat. 115-545-062, 1:100 dilution; Jackson Immuno Research Inc., West Grove, PA, USA). After washing with PBS three times, tumor slides were mounted using Prolong[®] Gold Antifade Reagent with 4',6-diamidino-2-phenylindole (DAPI, Invitrogen, Carlsbad, CA, USA) and cover glass. Confocal laser scanning microscopy was performed using a FV1200 confocal microscope (Olympus) with a 60 \times oil immersion lens. All photographs were taken with the same exposure time. Brightness and contrast adjustments were made equally for all images.

In vivo fluorescent imaging and tumor removal in mice with peritoneal carcinomatosis

To evaluate whether Tc-99m Folate-ECG-ROX could efficiently enable visualization of tumor tissue and guide surgery during operation, surgical removal of tumor tissue was performed. Mice with peritoneal carcinomatosis were prepared by

intra-peritoneal injection of 1×10^7 KB cells (0.1 ml PBS). On day 10, mice with peritoneal carcinomatosis were anesthetized by intra-peritoneal injection of ketamine (60 mg/kg)/xylazine (5 mg/kg). Then, 55.5 MBq (200 nM in 150 μl) of Tc-99m Folate-ECG-ROX was intravenously administered via tail vein. At 3 h after injection, surgical removal of the tumor tissue was performed under the field of view of the fluorescence-imaging system. After tumor removal, optical imaging was performed for the carcass and excised tumor nodules. Immunohistochemistry staining with anti-FR antibody for excised tumor nodules was performed as described above.

Statistical analysis

Data are presented as means \pm standard deviation (SD). Target to non-target ratios obtained from gamma camera imaging and competition studies were compared using one-way analysis of variance and appropriate post hoc tests. A p value < 0.05 was considered statistically significant. All data analyses were performed using SPSS version 18.0 (SPSS Inc., IBM Co., Armonk, NY, USA).

Ethical considerations

All animal experiments were performed in accordance with guidelines of the Wonkwang University School of Medicine Committee to minimize the pain and killing of the animals.

Results

Synthesis of Folate-ECG-ROX and radiolabeling with Tc-99m

Folate-ECG-ROX ($\text{C}_{83}\text{H}_{95}\text{N}_{21}\text{O}_{21}\text{S}_1$, Mol. Wt.: 1754.83) was successfully synthesized using Fmoc SPPS (Fig. 1). A single radiocompound was obtained by RP-HPLC (retention time = 22.4 min) after Tc-99m radiolabeling. The Tc-99m Folate-ECG-ROX complex was prepared in high yield ($> 97\%$). It showed high stability in saline and serum. Intact percentages of Tc-99m Folate-ECG-ROX incubated in saline measured by ITLC-SG were 97.1 ± 0.4 , 96.5 ± 0.5 , 94.8 ± 0.8 , and $92.7 \pm 1.5\%$ at 30 min, 1, 3, and 24 h, respectively. Intact percentages of Tc-99m Folate-ECG-ROX incubated in serum were 96.2 ± 0.8 , 96.2 ± 0.7 , 93.7 ± 1.2 , and $91.6 \pm 1.7\%$ at 30 min, 1, 3, and 24 h, respectively.

In vitro receptor-binding affinity and cellular uptake

K_d of Tc-99m Folate-ECG-ROX for KB cells was estimated to be 6.9 ± 0.9 nM (Supplemental Data 1A). In contrast, the K_d of Tc-99m Folate-ECG-ROX for HT-1080

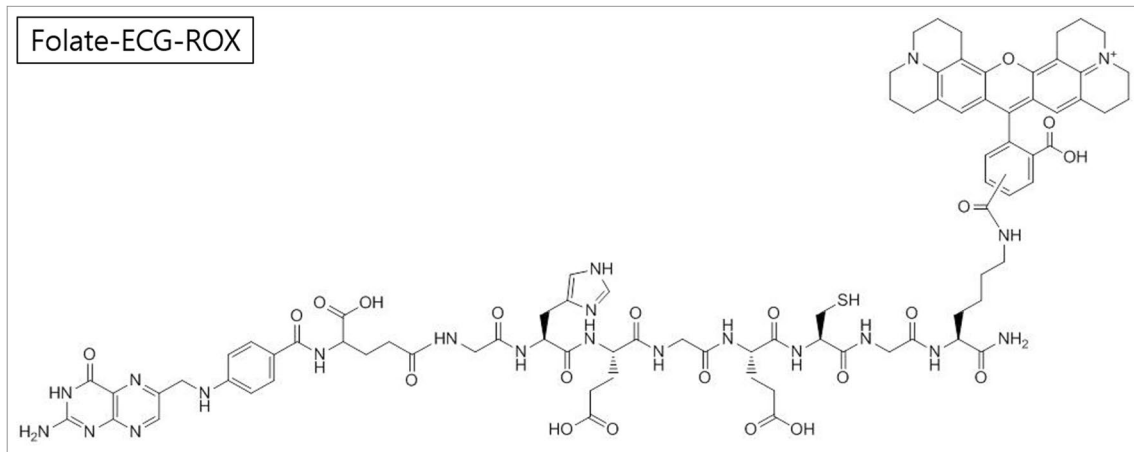


Fig. 1 Chemical structure of Folate-ECG-ROX

cells was estimated to be 4340 ± 3352 nM (Supplemental Data 1B), which was significantly higher than that for KB cells ($p < 0.005$). These results demonstrate that Tc-99m Folate-ECG-ROX shows high affinity for FR-specific uptake.

Confocal microscopy images of KB cells incubated with Folate-ECG-ROX revealed strong fluorescence activity of ROX in cell membrane and cytoplasm (Fig. 2a). In contrast, the fluorescence activity of ROX was barely detectable in HT-1080 cells incubated with Folate-ECG-ROX (Fig. 2b).

In vivo gamma camera imaging and competition study

In mice, the most intense activity was observed in the kidneys, suggesting that Tc-99m Folate-ECG-ROX was mainly excreted through the renal systems. It also indicates FR expression in the kidneys. Tc-99m Folate-ECG-ROX accumulated substantially in FR-positive KB tumors (Fig. 3a, arrows). Tumor to normal muscle uptake ratio of Tc-99m Folate-ECG-ROX increased with time (3.4 ± 0.4 ,

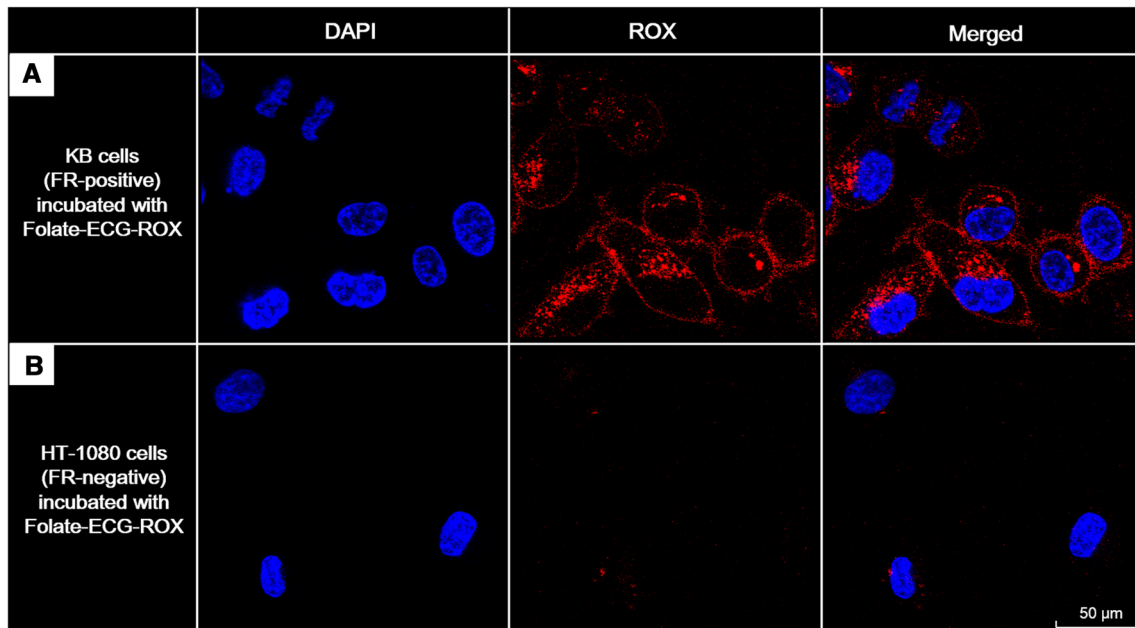


Fig. 2 Confocal microscopy images of folate receptor (FR)-positive KB cells incubated with Folate-ECG-ROX showed strong fluorescence activity in the cytoplasm (a). In contrast, FR-negative HT-1080 cells showed weak fluorescence activity of ROX (b)

4.4 ± 0.7 , and 6.6 ± 0.8 at 1, 2, and 3 h, respectively). In contrast, Tc-99m Folate-ECG-ROX did not significantly accumulate in FR-negative HT-1080 tumors (Fig. 3a, arrow heads). Tumor to normal muscle uptake ratios (1.9 ± 0.3 , 1.9 ± 0.5 , and 2.2 ± 0.5 at 1, 2, and 3 h, respectively) were significantly lower than those of KB tumors ($p < 0.05$, Fig. 4).

In the competition study, when excess folate and Tc-99m Folate-ECG-ROX were co-injected, the uptake of KB tumor was significantly decreased (tumor to normal muscle uptake ratios: 2.6 ± 0.3 , 2.9 ± 0.5 , and 2.8 ± 0.3 at 1, 2, and 3 h, respectively, Fig. 3b, arrows). These observations indicated that co-injection of excess folate could inhibit the uptake of Tc-99m Folate-ECG-ROX into KB tumors ($p < 0.05$, Fig. 4).

Ex vivo fluorescent imaging, biodistribution and immunohistochemistry staining

In ex vivo fluorescent images, high fluorescent activity of Tc-99m Folate-ECG-ROX was detected in the kidney among healthy organs (Fig. 5). Significant fluorescent

activity of ROX was detected in KB tumor (arrow) while weak fluorescent activity was detected in HT-1080 tumor (arrow head). These observations were strongly correlated with in vivo gamma camera images.

At 1 and 3 h after injection of Tc-99m Folate-ECG-ROX, %IA/g biodistribution values are summarized in Table 1. At 1 h, kidneys showed the highest activity (20.03 ± 6.54). At 3 h, the activity of normal organs except kidneys decreased, representing washout of unbound Tc-99m Folate-ECG-ROX. Values of %IA/g for KB tumor (2.50 ± 0.80 and 4.08 ± 1.16 at 1 and 3 h, respectively) were significantly higher than those of HT-1080 tumor (0.94 ± 0.93 and 0.78 ± 0.25 at 1 and 3 h, respectively). In FR-positive KB tumor, tumor to normal muscle ratios of %IA/g values were 3.1 ± 2.7 and 7.4 ± 3.2 for Tc-99m Folate-ECG-ROX at 1 and 3 h, respectively.

Confocal microscopy with immunohistochemistry staining detected strong Tc-99m Folate-ECG-ROX fluorescence within KB tumor tissue. The fluorescence was correlated with the fluorescent activity of anti-FR antibody (Fig. 6a). However, fluorescent activity of ROX and anti-FR antibody was weakly detected in the HT-1080 tumor tissue (Fig. 6b).

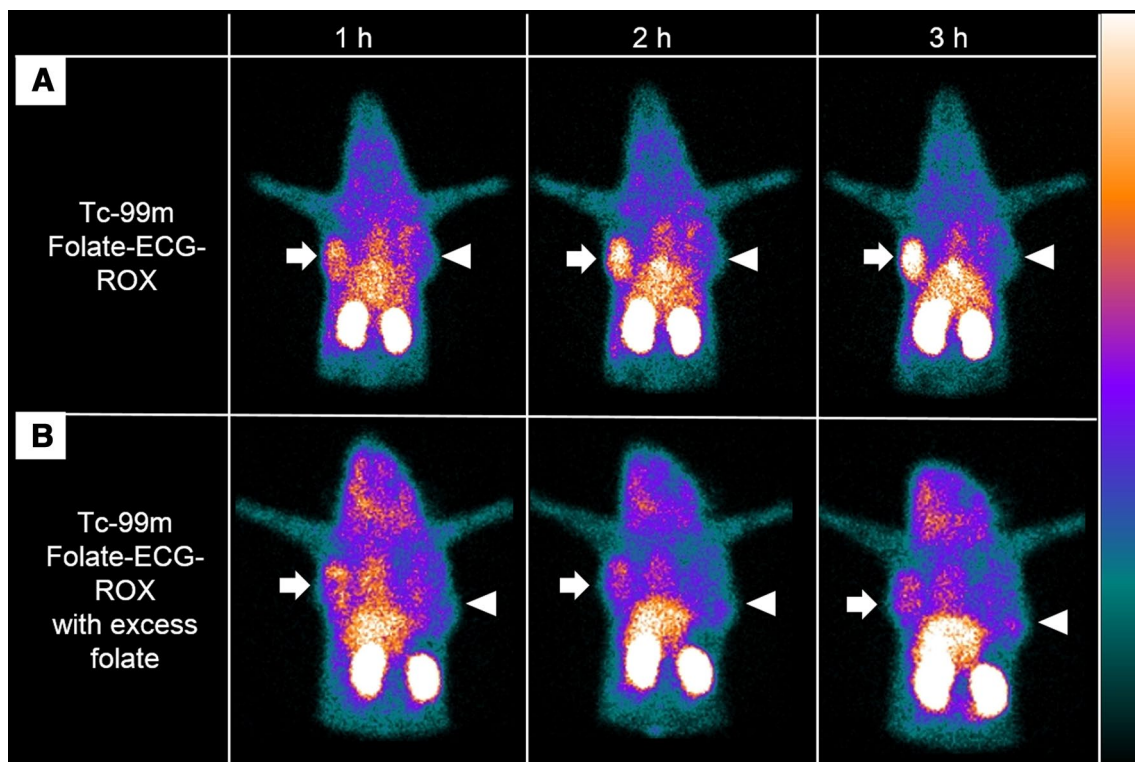


Fig. 3 **a** After injection of Tc-99m Folate-ECG-ROX, serial gamma camera imaging of tumor-bearing mice revealed substantial uptake in the KB tumor (arrows). In contrast, HT-1080 tumor (arrow heads)

showed relatively low uptake of Tc-99m Folate-ECG-ROX. **b** Co-injection of excess concentration folate reduced tumor uptake of Tc-99m Folate-ECG-ROX

Fig. 4 At 1, 2 and 3 h after injection of Tc-99m Folate-ECG-ROX, tumor to normal muscle uptake ratios of KB tumors were significantly higher than those of HT-1080 tumors and tumors with co-injection of excess folate ($p < 0.05$, asterisks)

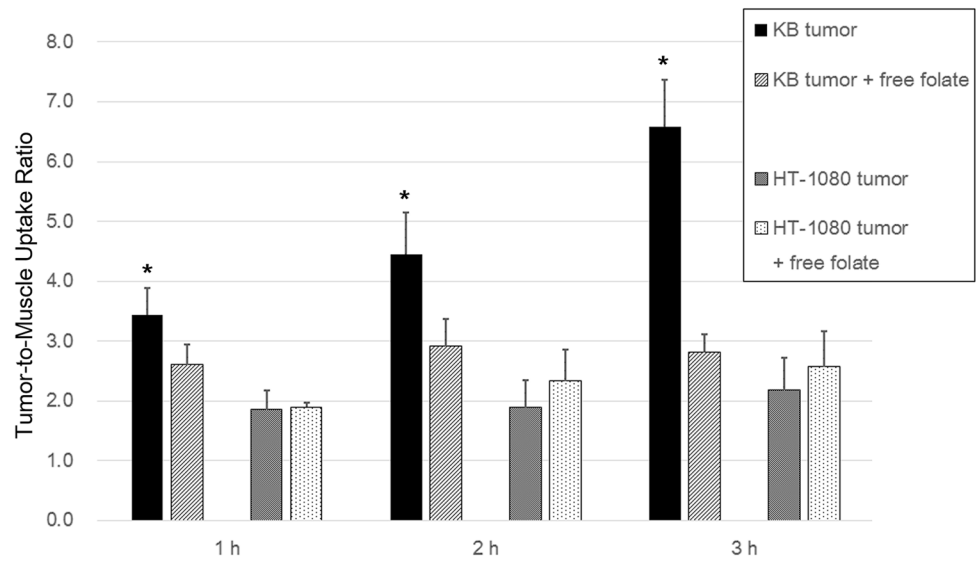


Fig. 5 On ex vivo optical images of excised organs, KB tumor showed significantly higher fluorescent activity of Tc-99m Folate-ECG-ROX (arrows) than HT-1080 tumor (arrow heads). (Lu, lung; Hr, heart; Sp, spleen; Lv, liver; St, stomach; Co, colon; Kd, kidney; Mu, muscle; KB, KB tumor; HT, HT-1080 tumor)

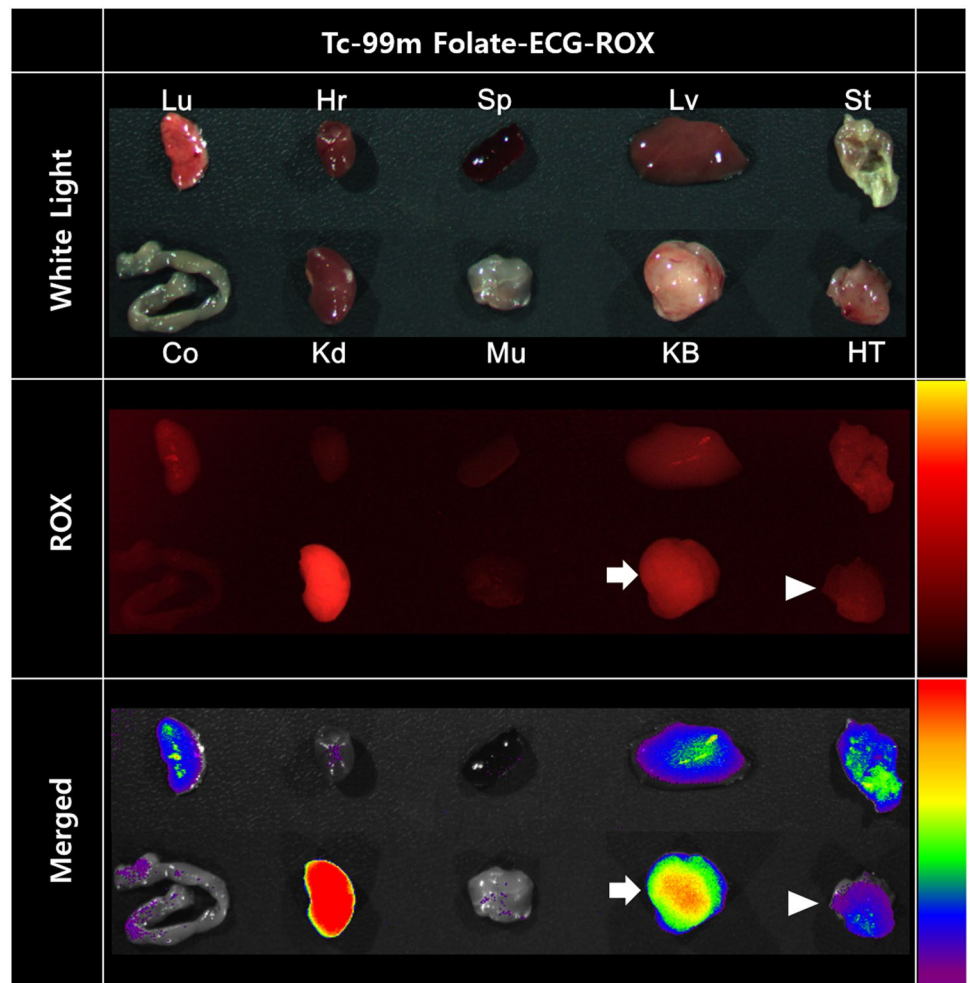


Table 1 Biodistribution data 1 and 3 h after injection of Tc-99m Folate-ECG-ROX in mice bearing KB and HT-1080 tumors

Organs	Mean %ID/g (SD)	
	1 h	3 h
Lungs	2.05 (0.48)	0.86 (0.18)
Heart	1.57 (0.43)	0.45 (0.16)
Blood	1.67 (0.24)	0.44 (0.17)
Liver	2.89 (1.35)	2.02 (0.82)
Stomach	2.27 (0.89)	2.11 (1.12)
Colon	1.25 (0.47)	0.35 (0.12)
Kidneys	20.03 (6.54)	10.52 (2.63)
Muscles	1.68 (1.61)	0.46 (0.10)
KB tumor (FR positive)	2.50 (0.80)	4.08 (1.16)
HT-1080 tumor (FR negative)	0.94 (0.93)	0.78 (0.25)

In vivo fluorescent imaging and tumor removal in mice with peritoneal carcinomatosis

Fluorescent images of mice with peritoneal carcinomatosis indicated that multiple tumor nodules were disseminated in the peritoneal cavity (Fig. 7a, arrows). Under real-time optical imaging, visible nodules were successfully removed (Supplemental Data 2). After removing superficially located peritoneal nodules, several tiny nodules were

left in the carcass (Fig. 7b). However, further operation was not performed to preserve the anatomy of mice. These extracted nodules showed substantially higher fluorescent activities than normal muscle (Fig. 7c). In immunohistochemistry staining with anti-FR antibody, all resected nodules had revealed FR-positive areas.

Discussion

We developed Tc-99m Folate-ECG-ROX as a dual-modality imaging agent for targeting FR-positive tumor. In vivo gamma imaging study demonstrated specific uptake of Tc-99m Folate-ECG-ROX into KB tumors. In a competition study, tumor uptake of Tc-99m Folate-ECG-ROX was effectively blocked by co-injection of excess free folate. Also, tumor uptake of Tc-99m Folate-ECG-ROX could be detected by ex vivo optical imaging and surgical removal of tumor nodules under optical camera was successfully performed.

Due to its highly disease-restricted expression pattern, FR is now well accepted as a promising receptor to develop targeted diagnostics and therapeutics for cancers [14]. Folate binds to the FR with high affinity and gets internalized via receptor-mediated endocytosis [15]. In the present study, confocal microscopy images of KB cells incubated with Folate-ECG-ROX showed that the fluorescence activity of ROX was mainly detected in the cell membrane and cytoplasm. These results were well correlated with the cellular uptake pathway of folate.

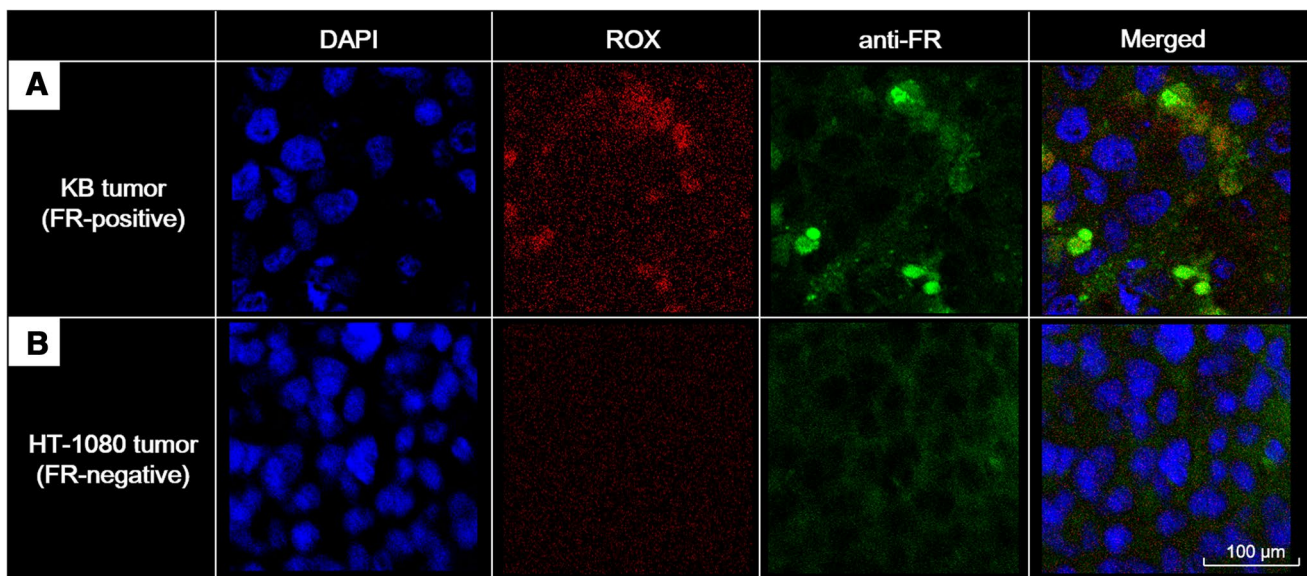


Fig. 6 On confocal microscopy with immunohistochemistry stain, strong fluorescent ROX activities of Tc-99m Folate-ECG-ROX were detected within KB tumor tissue, consistent with anti-folate receptor

antibody staining (a). HT-1080 tumor tissue showed relatively weak fluorescent activity of ROX and anti-folate receptor antibody (b)

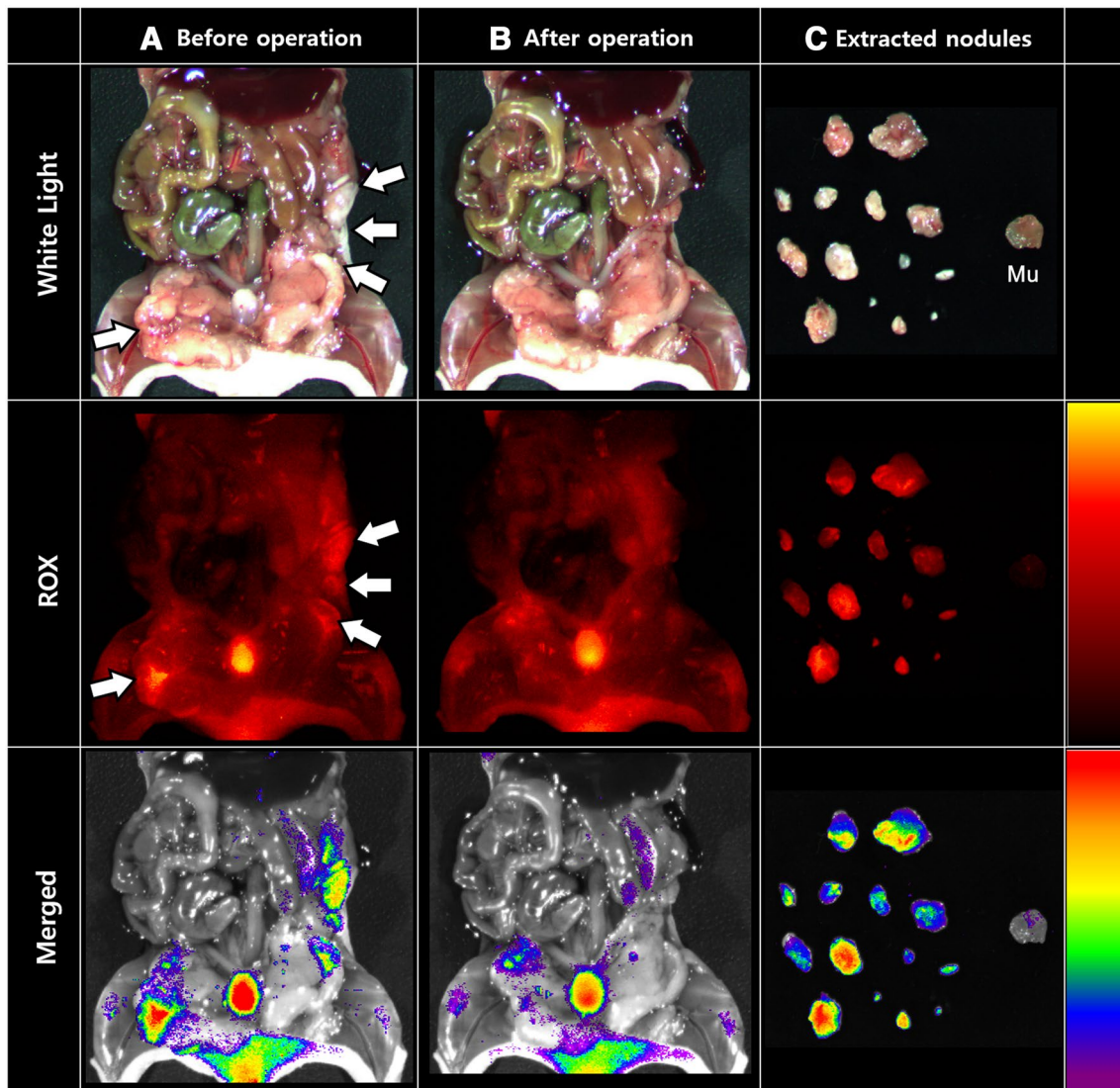


Fig. 7 Fluorescent images of mice with peritoneal carcinomatosis at 3 h after injection of Tc-99m Folate-ECG-ROX indicated that multiple tumor nodules were disseminated in the peritoneal cavity

(**a**, arrows). Under real-time optical imaging, visible nodules were removed (**b**). Extracted nodules showed relatively higher fluorescent activity than normal muscle (Mu, **c**)

One of the most successful folate radioconjugates is Tc-99m etarfolatide (EC20). It is currently undergoing clinical trials [16, 17]. Tc-99m EC20 showed high tumor uptake (17.2%IA/g) in a mouse model with FR-positive syngeneic M109 tumors [18]. However, this molecule could only be used for gamma imaging. Uptake of Tc-99m EC20 by KB tumors and FR-positive M109 syngeneic tumors were shown to be 8.92 and 15.02%IA/g, respectively, suggesting lower uptake of Tc-99m EC20 by KB tumors than that by M109 syngeneic tumors [19]. The uptake of Tc-99m EC20 by KB tumors (8.92%IA/g at 4 h after injection) was higher than that of Tc-99m Folate-ECG-ROX (4.08%IA/g at 3 h after injection). However, the time point of killing was different and tumor to kidney ratio obtained with Tc-99m

Folate-ECG-ROX (0.39) was higher than that obtained with Tc-99m EC20 (0.15).

Surgery is an effective method to remove solid tumors, with > 50% of cancer patients undergoing surgery each year [20]. Failure to obtain complete disease clearance due to incomplete resection is a major challenge in tumor surgery. It occurs in 20–60% of operations [20]. Although various clinical imaging modalities have been developed to visualize internal body structures and detect abnormal tissues prior to surgical procedures, most medical imaging modalities do not provide disease-specific images in real time [21]. In response to this unmet clinical need, optical imaging provides real-time visualization of the surgical field, especially when it is combined with fluorescent dye, allowing intra-operative

image-guided surgery. Nevertheless, only two fluorescent probes, methylene blue and indocyanine green, have been used for clinical use [22]. Unfortunately, these two fluorescent dyes are not cancer specific. They are passively accumulated in tumors [23]. It is important to note that the ability to visualize a target tissue mainly depends on the optical contrast due to difference amount of molecular uptake into target and normal tissues [24]. To achieve high target to background ratio, fluorescent agent needs to have cancer specificity. Dam et al. [4] have reported intra-operative tumor-specific fluorescence imaging with an FR-targeted fluorescent agent showcasing its potential applications in patients with ovarian cancer for improved intra-operative staging and more radical cytoreductive surgery. However, the development of FR-targeted multimodality imaging agent is limited. To the best of our knowledge, this is the first study to develop FR-targeting multimodality imaging agent containing both Tc-99m and fluorescence dye. The present study demonstrates that Tc-99m Folate-ECG-ROX have substantial specificity for FR-positive cancer cells and tissues.

Near-infrared (NIR) fluorescent dyes such as Cy 5.5 and Cy 7.0 with longer emission wavelength could provide better tissue penetration in vivo. However, these fluorescent dyes suffer from poor water solubility. Thus, incorporation of these fluorescent dyes into peptide sequence can severely compromise water solubility [25]. High water solubility is crucial for biocompatibility, high uptake efficiency, and low toxicity. It is an important chemical characteristic of molecular imaging agent [26]. Thus, we decided to use ROX as the fluorescent dye to increase water solubility. ROX is adequate for ex vivo imaging and intra-operative guidance in this study.

The ECG sequence of Folate-ECG-ROX, a tripeptide including multiple nitrogen and single sulfur atoms showed strong and stable chelation with Tc-99m. It is considered a good candidate for Tc-99m-chelating ligand [9–11]. We decided to insert histidine-containing sequence, GHEG, between folate and ECG-ROX as a linker or spacer. King et al. [27] have proposed that the histidine could displace one ligand from another and that additional distance between two ligands could reduce the effect or disturbance of ECG-ROX on the targeting ability of folate.

This study has several limitations. Unfortunately, nuclear and fluorescent imaging was not performed simultaneously in this study. Since each imaging is performed at different time point, there could be a concern that the advantage of dual imaging agent over combination of two single modal nuclear and fluorescent imaging agents is uncertain. However, a single injection of our dual-modality imaging agent enables imaging from whole body, tissue and down to cellular level. We had tried to demonstrate this benefit in nuclear imaging, fluorescent imaging and immunohistochemistry

staining studies. In the further study, the simultaneous nuclear and fluorescent imaging should be performed using commercially available multi-modal imaging device. Second, binding affinity and tumor accumulation of Tc-99m Folate-ECG-ROX was lower than those of previously reported single modal agent, Tc-99m folate-GGCE [28]. K_d value of Tc-99m Folate-ECG-ROX and Tc-99m folate-GGCE was 6.9 and 5.2 nM, respectively. Since the molecular weight of 5-ROX (Wt.: 528) is larger than that of folate (Wt.: 477), binding of folate on FR might be disturbed by 5-ROX. More effective spacer other than GHEG should be incorporated in the further study.

Conclusions

We developed Tc-99m Folate-ECG-ROX as a dual-modality imaging agent targeting FR of tumor. In vivo and in vitro studies demonstrated substantial and specific affinity of Tc-99m Folate-ECG-ROX for FR. Nuclear imaging using Tc-99m could allow quantitative assessment of organ distribution and tumor accumulation while fluorescent imaging using ROX could provide microscopic, ex vivo, and in vivo fluorescent imaging. Thus, Tc-99m Folate-ECG-ROX could provide both pre-operative molecular imaging and intra-operative guidance. Its feasibility was simulated in murine models. Taken together, results of the present study suggest that Tc-99m Folate-ECG-ROX is a potential dual-modality imaging agent for diagnosis and surgical guidance of FR-positive tumor.

Acknowledgements This work was supported by Basic Science Research Program and National Nuclear R&D Program through the National Research Foundation of Korea (NRF) funded by the by the Ministry of Science and ICT (2017R1C1B2001886 and 2019M2D2A1A01032296).

Compliance with ethical standards

Conflict of interest The authors declare that they have no conflict of interest.

References

1. Cai W, Chen X. Multimodality molecular imaging of tumor angiogenesis. *J Nucl Med.* 2008;49(Suppl 2):113S–S12828.
2. Li C, Wang W, Wu Q, Ke S, Houston J, Sevic-Muraca E, et al. Dual optical and nuclear imaging in human melanoma xenografts using a single targeted imaging probe. *Nucl Med Biol.* 2006;33:349–58.
3. Ghosh SC, Azhdarinia A. Advances in the development of multimodal imaging agents for nuclear/near-infrared fluorescence imaging. *Curr Med Chem.* 2015;22:3390–404.
4. van Dam GM, Themelis G, Crane LM, Harlaar NJ, Pleijhuis RG, Kelder W, et al. Intraoperative tumor-specific fluorescence

- imaging in ovarian cancer by folate receptor- α targeting: first in-human results. *Nat Med*. 2011;17:1315–9.
5. Metildi CA, Hoffman RM, Bouvet M. Fluorescence-guided surgery and fluorescence laparoscopy for gastrointestinal cancers in clinically-relevant mouse models. *Gastroenterol Res Pract*. 2013;2013:290634.
 6. Hall NC, Plews RL, Agrawal A, Povoski SP, Wright CL, Zhang J, et al. Intraoperative scintigraphy using a large field-of-view portable gamma camera for primary hyperparathyroidism: initial experience. *Biomed Res Int*. 2015;2015:930575.
 7. Parker N, Turk MJ, Westrick E, Lewis JD, Low PS, Leamon CP. Folate receptor expression in carcinomas and normal tissues determined by a quantitative radioligand binding assay. *Anal Biochem*. 2005;338:284–93.
 8. Fani M, Wang X, Nicolas G, Medina C, Raynal I, Port M, et al. Development of new folate-based PET radiotracers: preclinical evaluation of (6)(8)Ga-DOTA-folate conjugates. *Eur J Nucl Med Mol Imaging*. 2011;38:108–19.
 9. Kim DW, Kim WH, Kim MH, Kim CG. Novel Tc-99m labeled ELR-containing 6-mer peptides for tumor imaging in epidermoid carcinoma xenografts model: a pilot study. *Ann Nucl Med*. 2013;27:892–7.
 10. Kim DW, Kim WH, Kim MH, Kim CG. Synthesis and evaluation of novel Tc-99m labeled NGR-containing hexapeptides as tumor imaging agents. *J Labelled Comp Radiopharm*. 2015;58:30–5.
 11. Kim DW, Kim WH, Kim MH, Kim CG. Synthesis and evaluation of Tc-99m-labeled RRL-containing peptide as a non-invasive tumor imaging agent in a mouse fibrosarcoma model. *Ann Nucl Med*. 2015;29:779–85.
 12. Wu C, Wei J, Gao K, Wang Y. Dibenzothiazoles as novel amyloid-imaging agents. *Bioorg Med Chem*. 2007;15:2789–96.
 13. Leamon CP, Reddy JA, Dorton R, Bloomfield A, Emsweller K, Parker N, et al. Impact of high and low folate diets on tissue folate receptor levels and antitumor responses toward folate-drug conjugates. *J Pharmacol Exp Ther*. 2008;327:918–25.
 14. Low PS, Henne WA, Doorneweerd DD. Discovery and development of folic-acid-based receptor targeting for imaging and therapy of cancer and inflammatory diseases. *Acc Chem Res*. 2008;41:120–9.
 15. Leamon CP, Jackman AL. Exploitation of the folate receptor in the management of cancer and inflammatory disease. *Vitam Horm*. 2008;79:203–33.
 16. Yamada Y, Nakatani H, Yanaihara H, Omote M. Phase I clinical trial of 99mTc-etarfolatide, an imaging agent for folate receptor in healthy Japanese adults. *Ann Nucl Med*. 2015;29:792–8.
 17. Morris RT, Joyrich RN, Naumann RW, Shah NP, Maurer AH, Strauss HW, et al. Phase II study of treatment of advanced ovarian cancer with folate-receptor-targeted therapeutic (vintafolide) and companion SPECT-based imaging agent (99mTc-etarfolatide). *Ann Oncol*. 2014;25:852–8.
 18. Leamon CP, Parker MA, Vlahov IR, Xu LC, Reddy JA, Vetzal M, et al. Synthesis and biological evaluation of EC20: a new folate-derived, (99m)Tc-based radiopharmaceutical. *Bioconj Chem*. 2002;13:1200–10.
 19. Muller C, Reddy JA, Leamon CP, Schibli R. Effects of the antifolates pemetrexed and CB3717 on the tissue distribution of (99m)Tc-EC20 in xenografted and syngeneic tumor-bearing mice. *Mol Pharm*. 2010;7:597–604.
 20. Aliperti LA, Predina JD, Vachani A, Singhal S. Local and systemic recurrence is the Achilles heel of cancer surgery. *Ann Surg Oncol*. 2011;18:603–7.
 21. Gibbs SL. Near infrared fluorescence for image-guided surgery. *Quant Imaging Med Surg*. 2012;2:177–87.
 22. Jiang JX, Keating JJ, Jesus EM, Judy RP, Madajewski B, Venegas O, et al. Optimization of the enhanced permeability and retention effect for near-infrared imaging of solid tumors with indocyanine green. *Am J Nucl Med Mol Imaging*. 2015;5:390–400.
 23. Xiao Q, Chen T, Chen S. Fluorescent contrast agents for tumor surgery. *Exp Ther Med*. 2018;16:1577–85.
 24. Lee JH, Park G, Hong GH, Choi J, Choi HS. Design considerations for targeted optical contrast agents. *Quant Imaging Med Surg*. 2012;2:266–73.
 25. Bouteiller C, Clave G, Bernardin A, Chipon B, Massonneau M, Renard PY, et al. Novel water-soluble near-infrared cyanine dyes: synthesis, spectral properties, and use in the preparation of internally quenched fluorescent probes. *Bioconj Chem*. 2007;18:1303–17.
 26. Jabir NR, Tabrez S, Ashraf GM, Shakil S, Damanhoury GA, Kamal MA. Nanotechnology-based approaches in anticancer research. *Int J Nanomed*. 2012;7:4391–408.
 27. King R, Surfraz MB, Finucane C, Biagini SC, Blower PJ, Mather SJ. 99mTc-HYNIC-gastrin peptides: assisted coordination of 99mTc by amino acid side chains results in improved performance both in vitro and in vivo. *J Nucl Med*. 2009;50:591–8.
 28. Kim WH, Kim CG, Kim MH, Kim DW, Park CR, Park JY, et al. Preclinical evaluation of isostructural Tc-99m- and Re-188-folate-Gly-Gly-Cys-Glu for folate receptor-positive tumor targeting. *Ann Nucl Med*. 2016;30:369–79.

Publisher's Note Springer Nature remains neutral with regard to jurisdictional claims in published maps and institutional affiliations.